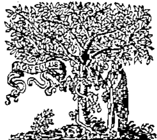

ELSEVIER

Materials Science and Engineering B35 (1995) 472–478

MATERIALS SCIENCE & ENGINEERING B

Real-time monitoring of heteroepitaxial growth processes on the silicon(001) surface by p-polarized reflectance spectroscopy

Klaus J. Bachmann[a,b,*], Uwe Rossow[c], Nikolaus Dietz[a]

[a] *Department of Materials Science and Engineering, North Carolina State University, Raleigh, NC 27695-7919, USA*
[b] *Department of Chemical Engineering, North Carolina State University, Raleigh, NC 27695-7919, USA*
[c] *Department of Physics, North Carolina State University, Raleigh, NC 27695-7919, USA*

Abstract

In this paper we describe the real-time monitoring by p-polarized reflectance spectroscopy (PRS) using pulsed chemical beam epitaxy (PCBE) of $Ga_xIn_{1-x}P$ on Si(001) as an example. For constant source vapor pulse height, width and repetition rate, the formation of the heteroepitaxial film on the Si(001) surface proceeds via a three-dimensional nucleation and overgrowth mechanism. Provision of a high initial supersaturation of the surface drives the nucleation kinetics toward a two-dimensional mechanism. The analysis of the fine structure in the PRS intensity reveals that under the conditions of quasi-steady state growth the surface chemistry cycles between enhanced and diminished P-activity and diminished and enhanced Ga-activity, with the dealkylation of the group III alkyl source molecules constituting a rate limiting step in the growth kinetics. Since the deposition rate per precursor pulse cycle can be determined experimentally, molecular layer epitaxy conditions can be imposed and verified in real-time without reliance on a self-limiting growth mechanism.

Keywords: Real-time optical process monitoring; Kinetics of heteroepitaxy; Gallium–indium phosphide on silicon(001); Engineered molecular layer epitaxy

1. Introduction

Real-time process monitoring is essential for interface engineering, in general, and the control of the local stoichiometry and structural perfection of heterostructures of small dimensions, in particular, since it permits the verification of reproducible initial surface conditions and the detection and correction of deviations from the desired nucleation and overgrowth kinetics during early stages of heteroepitaxy. For the growth of $Ga_xIn_{1-x}P$ epilayers on Si(001) by pulsed chemical beam epitaxy (PCBE), pulsed ballistic beams of triethylgallium (TEG), trimethylindium (TMI), tertiarybutylphosphine (TBP), and a steady flux of activated hydrogen are directed onto the hot surface of the substrate in computer-controlled time sequence. p-Polarized reflectance spectroscopy (PRS) is based on the changes in the reflectivity during the formation of a heteroepitaxial stack with regard to a beam of p-polarized light that impinges onto the surface at the Brewster angle of the substrate. It provides for the real-time monitoring of (i) the initial surface temperature and cleanliness, (ii) the rate of film growth, (iii) the bulk optical properties of the film, (iv) the nucleation and overgrowth kinetics and (v) the kinetics of heteroepitaxial growth under steady state conditions.

2. Real-time monitoring of PCBE of $Ga_xIn_{1-x}P$ on Si(001) by PRS

In this paper we describe a single wavelength application of PRS using a chopped beam of HeNe laser light of 632.8 nm wavelength. It is polarized by means of a Glan–Thompson polarizer to a ratio of the s- and p-polarized components of the incident intensity $I_s/I_p \approx 10^{-6}$ corresponding to a residual reflectivity of about 10^{-4}. The reflected radiation is detected by a

* Corresponding author.

0921-5107/95/$09.50 © 1995 — Elsevier Science S.A. All rights reserved

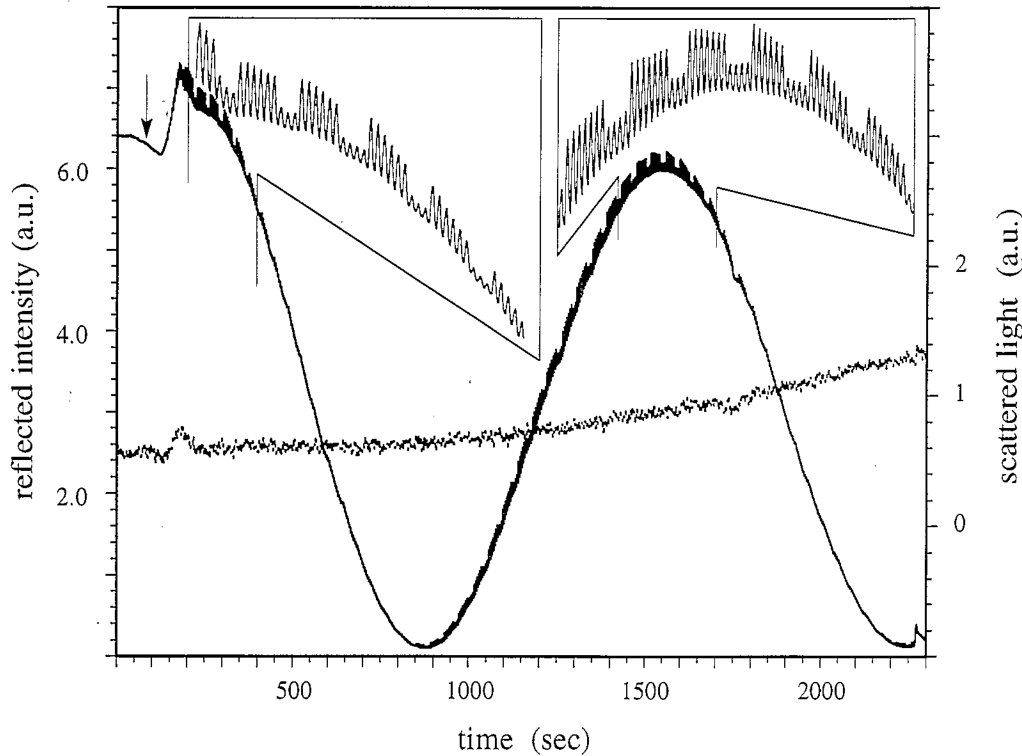

Fig. 1. Interference fringes in the PRS intensity vs. time traces observed during PCBE growth of GaP on Si(001). The arrow marks the start of PCBE.

photodiode, the output of which is processed through a phase sensitive amplifier and read into a computer. Also, the radiation that is scattered by the growing film into a solid angle of 5° is focused by a lens at a location well-removed from the plane of incidence of the impinging light beam onto the entrance slit of a photomultiplier. Laser light scattering (LLS) provides information on the roughness of the top and bottom interfaces of the film. For further details of the experimental arrangement for PCBE [1] with optical process monitoring by PRS [2] and its combination with reflectance difference spectroscopy (RDS) [3] we refer the reader to Ref. [4].

Under the above described experimental conditions, the complex reflectivity coefficient r_p of a three-layer stack—composed of materials labeled a, b and c with interfaces labeled a/b and b/c—is given by

$$r_p = \frac{r_{a/b} + r_{b/c}\exp(-2i\Phi)}{1 + r_{a/b}r_{b/c}\exp(-2i\Phi)} \tag{1}$$

where $r_{a/b}$ and $r_{b/c}$ are the Fresnel reflection coefficients for the interfaces a/b (ambient/film) and b/c (film/substrate) for p-polarized light.

$$\Phi = \frac{2\pi t_b}{\lambda}(\epsilon_b - \epsilon_a \sin^2\varphi_o)^{1/2} \tag{2}$$

is the film phase factor which depends on the film thickness t_b, the angle of incidence φ_o, and the dielectric functions of the ambient ϵ_a and of the film ϵ_b at the frequency of the incident electromagnetic wave of wavelength λ.

Uniform heteroepitaxial growth of the III–V compounds on Si(001) requires heating of the initially hydrogen terminated surface to the process temperature (typically about 350 °C) under steady fluxes of both TBP and hydrogen. The change in the reflectivity of the substrate—related to the temperature dependence of its dielectric function upon heating—allows a non-intrusive check on the reproduction of the chosen surface temperature in each experiment. Also, if the surface should become contaminated during heating to the growth temperature the concomitant changes in the dielectric properties are immediately detected. The monitoring of the surface properties prior to growth thus provides valuable information with regard to the reproducibility of the initial conditions for the growth process and the opportunity for early termination of the experiment in the event of contamination problems.

Fig. 1 shows the PRS intensity as a function of time for the growth of GaP on Si(001). The featureless first section of this trace marks the reflectivity of the phosphorus-terminated Si surface at the growth temperature. At the time indicated in Fig. 1 by an arrow TEG pulses are added to the TBP pulses with chosen pauses between the trailing and leading edges of (1) the TEG pulse and the following TBP pulse and (2) this TBP pulse and the following TEG pulse, thus initiating the PCBE process. Upon growth of the GaP epilayer the reflected intensity $R = r \cdot r^*$ oscillates due to interference in the film with maxima and minima at phase difference $2z\pi$ and $(2z+1)\pi$ between the partial waves reflected at

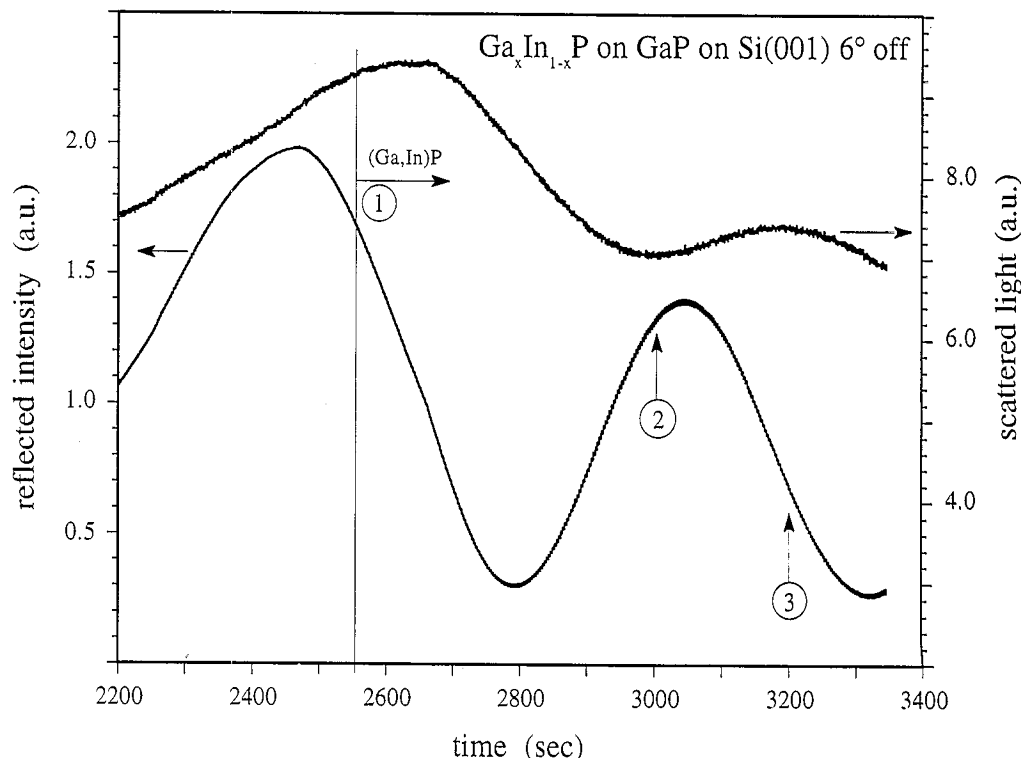

Fig. 2. PRS intensity vs. time trace for step-graded PCBE of $Ga_xIn_{1-x}P$ on a GaP coated Si(001) substrate. The arrows 1, 2, 3 mark steps in the TEG to TEG flux ratio: 1, $f_{TEG}:f_{TMI} = 5:1.2$; $f_{TEG}:f_{TMI} = 10:3.3$; $f_{TEG}:f_{TMI} = 5:2$.

the interfaces a/b and b/c respectively, z being an integer. The spacing between the minima in the PRS intensity is given by $\lambda/[2(\epsilon_a - \epsilon_b \sin^2\varphi_o)]^{1/2}$ and permits the calibration of the film thickness as a function of time, that is a real-time measurement of the growth rate.

Fig. 2 shows the PRS intensity as a function of time for the step-graded growth of $Ga_xIn_{1-x}P$ on Si(001). The growth process starts with PCBE of GaP and switches at the position of the arrow to step-graded growth of $Ga_xIn_{1-x}P$. Although the dielectric function increases with increasing In-content in the alloy, no significant discontinuities are observed in the PRS signal at the position of the increases in the TMI:TEG flux ratio marked by arrows in Fig. 2.

In addition to the quarter wavelength oscillations due to interference, a fine structure is observed in the PRS intensity which is shown in the inset in Fig. 2 at higher magnification. Fig. 3 shows the correlation between the fine structure in the PRS intensity and the pulse sequences employed in the steady state growth of (a) GaP and (b) $Ga_xIn_{1-x}P$ on Si(001) in the presence of a continuous beam of hot filament-activated hydrogen. Each peak in the fine structure corresponds to a complete precursor cycle with the leading edge in the periodic PRS intensity always coinciding with the leading edge of the first TBP pulse of the sequence. Note that whether this leading edge is associated with an increase or decrease in the reflectivity depends on time, i.e. its sign changes periodically in the course of the experiment for reasons entirely related to the optical properties of the evolving four-layer stack: substrate–epilayer–surface-layer–ambient [5]. The response to the second TBP pulse of sequence (b) is not resolved, but broadens the fine structure peaks. No pronounced feature in the PRS intensity develops at the time of exposing the surface to the group III–alkyl flux in either trace (a) or (b).

Table 1 lists the GaP growth rate per cycle under quasi-steady state growth conditions for pauses (1) and (2) of different lengths at fixed pulse widths W(TEG) = 0.2 s and W(TBP) = 0.8 s, heights H(TEG) = 0.06 sccm and H(TBP) = 0.5 sccm and substrate temperature T_s = 633 K. A comparison of the results of experiments 5 and 6 reveals that within the error of its determination (less than 5%) the growth rate is unaffected by the pause between the TBP and the following TEG pulses. However, the results of experiments 1–5 and 7 show clearly that the growth rate per cycle increases with increasing length of the pause between the TEG pulse and the following TBP pulse from nominally 1.20 to 3.43 Å/cycle for second pause duration changing from 0 to 3.6 s. Concomitantly, the position of the TEG pulse shifts with increasing length of the second pause toward the maximum in the PRS signal. We interpret these observations as the result of a kinetic barrier to the dealkylation of the impinging TEG molecules on the GaP surface, corresponding to a time constant of the order of 1 s for their conversion into surface species that contribute to the growth. Independent investigations of the decomposition kinetics on

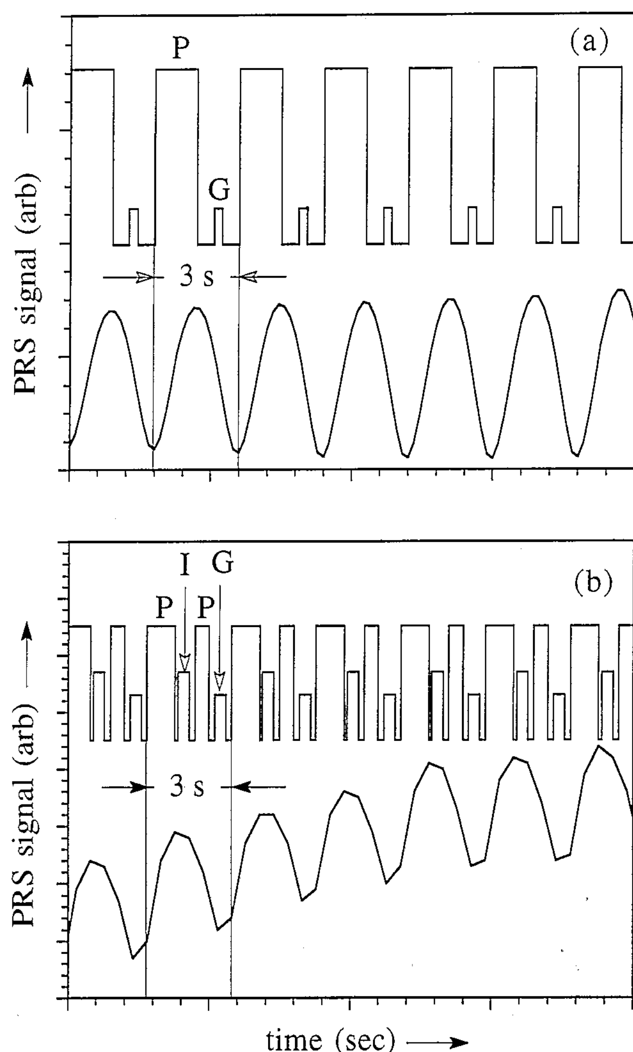

Fig. 3. Correlation of the fine structure in the PRS intensity vs. time traces and the timing of the source vapor pulses under the conditions of PCBE in quasi-steady state of (a) GaP on Si (001) and (b) $Ga_xIn_{1-x}P$ on Si(001).

GaAs [6,7] reveal molecular adsorption at low temperature (150 K) and the onset of partial decomposition upon heating below room temperature. Rapid ethane, hydrogen and ethene desorption is observed at 620–670 K. Although the decomposition kinetics of $Ga(C_2H_5)_3$ on a GaP surface is expected to differ somewhat from the behavior observed on GaAs, we expect that under the conditions of our experiments the TEG molecules arriving on the GaP surface break-up, resulting in a partial dealkylation that is further advanced by interactions with active hydrogen on the surface during the pause periods. Thus a reservoir of Ga-precursors in an inactive state coexists on the surface with active Ga precursors to growth.

This interpretation of the growth rate enhancement with increasing pause after the TEG pulse is further corroborated by interrupted growth experiments, where after establishing quasi-steady state growth conditions the TEG pulses are shut off, but the TBP flux is continued for some period after which the TEG pulses are added again. The response in the PRS intensity is shown in Fig. 4 for two different interruption periods Δt_i under the same experimental conditions (trace A: $\Delta t_i = 51$ s; trace B: $\Delta t_i = 18$ s). Note that during the interruption period the PRS intensity remains at the level of the maximum expected in the fine structure after the last TEG pulse plus one TBP pulse. Thus the maxima in the PRS during quasi-steady state growth shown in Fig. 4 correspond to nearly complete consumption of the active Ga-precursors to growth during exposure to the TBP pulse, cycling the surface between (I) supersaturation by active Ga-precursors before the arrival of the TBP pulse and (II) a surface depleted of active Ga-precursors to growth. Since the PRS intensity does not increase any further upon continuing exposure to the TBP flux in the absence of TEG pulses, the maxima in the PRS fine structure represent a surface that is close to the maximum attainable phosphorus activity at the chosen TBP flux. The slight decrease in the PRS intensity during interruption of the TEG flux to the surface may either be due to continuing growth that depletes the reservoir of inactive TEG fragments or changes in the experimental conditions unrelated to film growth. However, that the surface retains some mem-

Table 1
Growth rate response to changing the pauses between the leading and trailing edges of (1) the TBP and TEG pulses and (2) the TEG and TBP pulses for seven GaP–Si(001) PCBE experiments. The final refers to the amplitude modulation of the PRS fine structure, where observed

Experiment number	Sequence time (s)	Pause (1) (s)	Pause (2) (s)	Growth rate (Å s^{-1})	Growth rate (Å/cycle)	Repeat distance (cycles)
1	1	0.0	0.0	1.20	1.20	1 [a]
2	1.5	0.2	0.5	1.15	1.88	1 [a]
3	2	0.4	0.6	1.07	2.14	1 [a]
4	3	0.8	1.2	0.92	2.76	10
5	4	1.2	1.8	0.78	3.12	72
6	5	2.2	1.8	0.62	3.10	28
7	7	2.4	3.6	0.49	3.43	15

[a]No amplitude modulation in the fine structure.

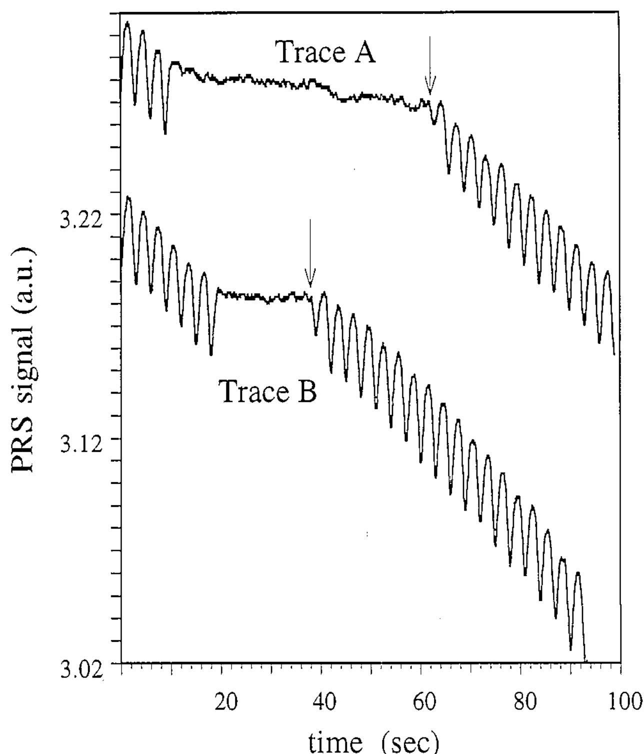

Fig. 4. PRS fine structure vs. time traces for interrupted PCBE of GaP. Trace A: no TEG pulses for 17 cycles; trace B: no TEG pulses for 6 cycles.

ory with regard to the last TEG exposure is revealed by the onset of PRS fine structure oscillations in traces A and B after resumption of the pulsed TEG flux to the surface. The time of the resumption of TEG pulse exposure of the surface is indicated by arrows. In the case of trace A the surface is essentially depleted of gallium of both active and inactive Ga-surface molecules so that upon admission of the first TEG pulse the PRS intensity is only slightly decreased. In trace B the memory of the preceding TEG exposure is still strong so that the resumption of the pulsed TEG flux results in a stronger deflection of the PRS intensity toward the minimum position under the conditions of quasi-steady state growth that is recovered in both traces A and B after the second TEG pulse.

In the case of homoepitaxy, the oscillations in the reflected intensity due to interference in the epilayer do not exist, but the fine structure persists, as illustrated in Fig. 2 for two GaP PCBE experiments establishing different growth rates per cycle. Note that the fine structure in both, the heteroepitaxy experiment of Fig. 1 and the homoepitaxy experiments of Fig. 5, exhibit an amplitude modulation and an additional envelope modulation at even lower frequency. The amplitude modulation depends on the height, width and repetition rate of the source vapor pulses and can be eliminated by an appropriate choice of these parameters. Where observed, the amplitude modulation repeats itself over extended periods of film growth in a characteristic sequence (see Fig. 1). For the GaP homoepitaxy fine structure traces A and B shown in fig. 5 these sequences are ...6 – 4 – 7 – 3 – 7 – 4 – 6 – 4 – 7 – 3 – 7 – 4 – 6 – 4... and ...2 – 1 – 2 – 2 – 2 – 1... corresponding to repeat distances of 72 and 10 cycles respectively. For the heteroepitaxial experiments considered in Table 1 amplitude modulation is observed in experiments 4 to 7. For these experiments, the repeat distance measured in number of cycles is listed. Note that for experiment 4, which corresponds to the conditions of trace B in the equivalent homoepitaxy experiment, close to a bilayer of GaP is deposited per cycle so that, with small adjustments in the length of the second pause, molecular layer epitaxy conditions can be engineered without need for a self-terminating mechanism, which is clearly absent under the conditions of our experiments.

During the initial period of nucleation and overgrowth of a substrate by a heteroepitaxial film the dielectric function must be replaced by an effective dielectric function

$$\epsilon_{eff} = \epsilon_a \frac{\epsilon_b(1+2p) + 2\epsilon_a(1-p)}{\epsilon_b(1-p) + \epsilon_a(2+p)} \qquad (4)$$

accounting for the corrugated structure of the film by the corrugation parameter $0 \leq p \leq 1$ [8]. The lower and upper limits of p correspond to the bare substrate surface and sealing of the substrate by a contiguous film respectively. The PRS intensity deviates thus in the critical initial stage of heteroepitaxy from the periodic signal predicted for constant bulk ϵ_b. Depending on the nucleation mechanism, the number of precursor cycles at which $p = 1$ may vary from a coverage of the Si surface by a single bilayer of the III–V compound for two-dimensional nucleation and over-growth (Frank–van der Merve mechanism) to several monolayers for

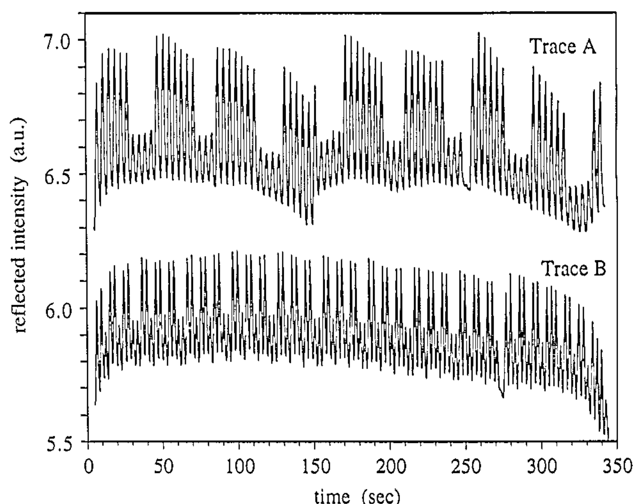

Fig. 5. Fine structure in the PRS intensity vs. time traces for (001) GaP homoepitaxy by PCBE at different growth rates. Trace A: 3.12 Å/cycle; trace B: 2.76 Å/cycle.

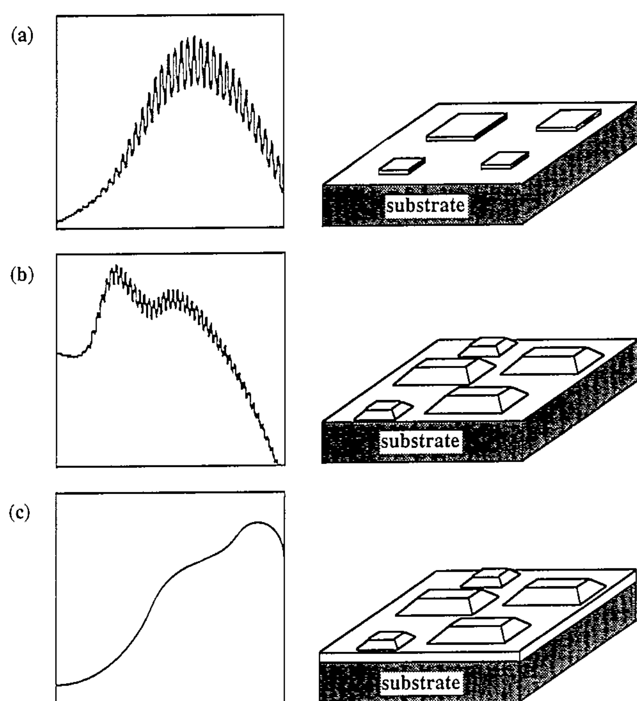

Fig. 6. Schematic representations of selected heteroepitaxial nucleation and overgrowth mechanisms (right side) and the associated PRS intensity vs. time traces (left side). (a) Frank–van der Merve mechanism, (b) Volmer–Weber mechanism, (c) Stranski–Krastanov mechanism. Traces (a) and (b) refer to experimental results for GaP nucleation on Si(001) under the conditions of PCBE. Trace (c) shows a schematic representation of a typical predicted PRS intensity variation with time.

the formation of nuclei of more than one III–V bilayers in height (Volmer–Weber mechanism), as illustrated in Figs. 6(a) and 6(b). That the condition $p = 1$ is reached at the junction of the excess intensity in the PRS signal to the interference oscillation of the reflected intensity is confirmed by atomic force microscopy (AFM)studies [9]. Owing to the catalytic enhancement of the TBP and TEG decomposition rates on the surface of the III–V surface elements [10] the corrugation depth—created by three-dimensional nucleation and overgrowth—is not determined by the thermodynamic definition of the habit of the nuclei, but is modified by the surface kinetics.

Through fine tuning of the precursor sequence during the initial period of PCBE the nucleation and overgrowth can be driven toward a two-dimensional mechanism as illustrated in Fig. 6(a). It involves starting at a higher TEG flux, which is decreased during the nucleation period to the same flux as used in the experiment, leading to the PRS trace shown in Fig. 6(b). The TBP fluxes in both experiments are the same. Recent investigations [11] by atomically resolved scanning tunneling microscopy (STM) show that, at moderate coverage, phosphine bonds at room temperature in molecular form via its lone pair to dimers on the Si(001) 2×1 surface breaking the weak π-bond. The adsorbed PH_3 sheds all its hydrogen atoms upon heating to 400 °C without substantial phosphorus desorption. Since the phosphorus atoms thus formed tend to replace Si dimer atoms to which the original bonding occurred the dominant surface species at moderate coverage are Si–P heterodimers. At high phosphine dose and elevated surface temperature the phosphorus concentration reaches nearly monolayer coverage [12–14], and the dominant surface species are P–P dimers, each atom carrying a lone pair [15]. Since the energy of the tert-butyl–phosphorus bond in the t-butPH_2 molecule is smaller than the energy required for cleaving the first hydrogen–phosphorus bond of PH_3, CBE growth of GaP on Si(001) using TEG and TBP becomes controlled by the decomposition kinetics of the source vapors at lower substrate temperature (about 260 °C) [16] than observed for the use of TEG and PH_3 (about 350 °C) [17]. Therefore, we expect under the conditions of our experiments a high phosphorus dimer concentration on the Si(001) surface just prior to admitting the first TEG pulse. In view of the shorter P–P dimer bond length, compared with the Si–Si bond length, the P-terminated surface is under tensile strain, which is further enhanced at the P–P dimer sites by bond angle distortions forced by the repulsion between the two lone pairs [15]. Thus electron deficient gallium atoms should bond readily to the P-surface atoms, while partially alkylated TEG fragments are less suited for reactions with surface phosphorus atoms. However, in view of the existing sink for surface gallium atoms and the high fluxes of both TBP and activated hydrogen (t-butyl radicals are known to be an excellent source of reactive surface hydrogen [18]), under the conditions of the experiment leading to the PRS intensity trace 5(a), the accelerated rate of dealkylation of the TEG fragments on the P-terminated Si(001) surface should result in a highly supersaturated surface, i.e. a higher frequency of nucleation than under the conditions of experiment leading to the PRS intensity trace 5(b). At large supersaturation the GaP nuclei are of small dimensions and form at a small average distance from each other so that they intergrow after a brief period of lateral growth. Also, both the enhanced Ga coverage of the Si surface and the higher density of GaP nuclei contribute to the realization of a more uniform surface kinetics, thus contributing to the observed trends in the nucleation mechanism upon fine tuning of the source vapor fluxes.

The transition from an initially two-dimensional overgrowth mechanism to corrugated film growth (Stranski–Krastanov mechanism) should be detectable by PRS as a delayed deviation of the intensity from the PRS signal expected for constant ϵ_b after sealing of the substrate by an initially planar contiguous heteroepitaxial film. This is illustrated schematically in Fig. 6(c). Of course, any surface roughening modifies the effective

dielectric function of the film. However, the magnitude of the deviation from ϵ_b scales with the ratio of the corrugation depth to the film thickness and thus is observable only if it occurs within a short period after the formation of a contiguous film. Therefore, a Stranski–Krastanov growth mechanism can be distinguished from surface roughening during later stages of film growth.

A detailed theoretical interpretation of the fine structure in the PRS intensity must incorporate both bulk and surface contributions to the dielectric function that are connected through modifications of the molecular orbitals of surface molecules by the backbonding to the solid and changes of the properties of the solid over several net planes by the surface modifications due to chemisorption of precursors to growth and products of the surface reactions. Such a theory does not exist at present, but further progress in the understanding of the changes in dielectric function in response to changes of the surface chemistry under the conditions of PCBE and of the associated PRS fine structure can be expected to emerge from the experimental correlation of the latter with the results of RDS and of in situ studies of the surface structure and bonding by AFM/STM and vibrational spectroscopies.

Acknowledgments

The work described in this paper has been supported by NSF grant DMR 9202210, the Office of Naval Research under contract ONR-00014-1-0255 and by the Alexander von Humboldt Foundation.

References

[1] J.T. Kelliher, J.T. Thornton, P.E. Russell and K.J. Bachmann, *MRS Symp. Proc.*, *317* (1993) 597.
[2] N. Dietz and K.J. Bachmann, *Mater. Res. Bull.*, *20* (5) (1995) 49.
[3] D.E. Aspnes, J.P. Harbison, A.A. Studna and L.T. Florez, *J. Vac. Sci. Technol. A*, *6*(3) (1988) 1327.
[4] N. Dietz, U. Rossow, D.E. Aspnes and K.J. Bachmann, *J. Electron. Mater.*, *24* (1995) 1569.
[5] N. Dietz and K.J. Bachmann, submitted to *Vacuum.*
[6] A.J. Murrell, A.T.S. Wee, D.H. Fairbrother, N.K. Singh, J.S. Foord, G.J. Davis and D.A. Andrews, *J. Cryst. Growth*, *105* (1990) 199.
[7] T. Maeda, J. Saito and K. Kondo, *J. Cryst. Growth*, *105* (1990) 191.
[8] J.C. Maxwell-Garnett, *Philos. Trans. R. Soc. London*, *203* (1904) 385; *Philos. Trans. R. Soc. London A*, *205* (1906) 237.
[9] E. Miller, N. Dietz and K.J. Bachmann, *MRS Symp. Proc.*, *355* (1995) 197.
[10] W. Richter, P. Kurpas, R. Lückerath, M. Motzkus and R. Waschbüsch, *J. Cryst. Growth*, *107* (1991) 13.
[11] Y. Wang, M.J. Bronikowski and R.J. Hamers, *J. Phys. Chem.*, *98* (1994) 5966.
[12] M.L. Yu and B.S. Meyerson, *J. Vac. Sci. Technol. A*, *2* (1984) 446.
[13] B.S. Meyerson and W. Olbricht, *J. Electrochem. Soc.*, *131* (1984) 2366.
[14] M.L. Yu, D.J. Vitkavage and B.S. Meyerson, *J. Appl. Phys.*, *59* (1986) 4032.
[15] Y. Wang, X. Chen and R.J. Hamers, *Phys. Rev. B*, *50* (1994) 4534.
[16] J.T. Kelliher, N. Dietz, J. Thornton, G. Lucovsky and K.J. Bachmann, *Mater. Sci. Eng. B*, *22* (1993) 97.
[17] M. Yoshimoto, K. Ozasa and H. Matsunami, *J. Appl. Phys.*, *70* (1991) 5708.
[18] S.H. Li, C.H. Chen, D.H. Jaw and G.B. Stringfellow, *Appl. Phys. Lett.*, *59* (1991) 2124.